

Low Profile Dual-Band Shared-Aperture Base Station Antennas based on FSS Radiators

H. Li, *Senior Member, IEEE*, J. Xu, Y. Nan, Q. Chen and C. Zhou

Abstract—In this letter, a low-profile dual-band dual-polarized base station antenna system is proposed for 5G applications. Distinct from previous base station antennas using FSS as a decoupling layer, the FSS structure is employed directly as the low band (LB) antenna at 0.69-0.96 GHz. At the same time, the FSS operates as the reflector for the high band (HB) antennas at 3.3-3.8 GHz. Hence, the radiation patterns of both the HB and the LB antennas are restored to match the patterns of the isolated antennas. Stable radiation and high boresight gains are achieved over the operating bands. The antennas are fabricated and measured, with the measurement results agreeing well with the simulated ones. The proposed antenna array is suitable for base stations with large-scale arrays due to its simple structure, low profile and stable radiation features.

Index Terms—Dual-polarized antennas, shared-aperture antennas, frequency selective surface (FSS), base station antennas, MIMO antennas.

I. INTRODUCTION

The fifth generation communication system has demonstrated the capacity to deliver extensive connectivity, high throughput, and low latency [1]-[6]. It becomes imperative to equip base stations with simultaneous support for 2G, 3G, and 4G/5G bands. Though a single antenna can cover dual or even multiple frequency bands [7]-[9], it is difficult to achieve stable radiation characteristics over all the bands. To provide constant radiation features, antennas of different dimensions are normally stacked together to operate at their fundamental resonances [10]-[16], yet resulting in high mutual coupling and high profile. Two popular arrangements for shared-aperture antenna arrays are depicted in Fig. 1(a) and (b), respectively. In Fig. 1(a), the HB antennas are located below the LB antennas, whereas the LB antenna is placed at the lower layer in Fig. 1(b). In both schemes, high isolations are in demand between the antennas at different bands.

Recently, decoupling methods have been extensively studied for shared-aperture antennas [17]-[30]. Once the low band antenna is placed at the upper layer [18]-[26], it is challenging to design the LB antenna as an electromagnetic transparent antenna at the HB. Various kinds of choke structures have been proposed to suppress the mutual coupling between the LB and the HB antennas, as shown in Fig. 1(c). In [18], a cascaded comb dipole antenna has been utilized in the LB to counteract the currents induced by the HB antenna, thereby suppressing the secondary radiation.

For the configuration with the HB antennas at the upper layer,

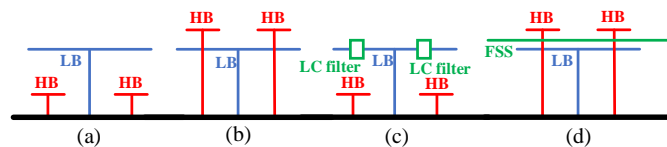


Fig. 1. Shared-aperture antenna structures: (a) LB-HB scheme; (b) HB-LB scheme; (c) LB-HB scheme with LC filter; (d) HB-LB scheme with FSS.

as shown in Fig. 1(b), the primary focus is on maintaining consistent reflection properties of the LB antenna for the HB antennas. The introduction of FSS structures is a common practice to achieve the reflection [27]-[30] and reduce the profile, as illustrated in Fig. 1(d). In [30], FSS has been initially employed to decouple the HB and LB antennas, effectively mitigating their interference. However, it is important to note that the placement of the FSS between the HB and LB antennas introduces certain complexities into the system and poses stability challenges.

In this article, the LB antenna is designed as an FSS surface to provide low transmission characteristics in the HB, so that the LB antenna acts as a ground plane for the HB antenna. This way, dual-layer dual-band shared-aperture antennas with restored radiation patterns are retained. The antenna array consists of a LB antenna at 0.69-0.96 GHz and four HB antennas at 3.3-3.8 GHz. Boresight radiations with the realized gains of 9 dBi and 8.3 dBi have been achieved, respectively, for the LB and the HB antennas. The lateral size of the antenna has been reduced by $0.2 \lambda_g$ compared with conventional FSS-based structures.

II. DUAL-BAND SHARED-APERTURE ANTENNAS

A. Antenna Configurations

Conventionally, the FSS structure is employed between the LB antenna and the HB antennas, achieving high-frequency stopband and low-frequency passband at the base station [27], [30]. In this scheme, a part of power radiated by the LB antenna is reflected by the FSS, resulting in a slightly lower efficiency of the LB antenna. Moreover, the antenna system becomes complicated with an extra FSS layer. In contrast, in this work, the FSS structure operates as the main radiator at the LB. Therefore, the number of the layers is reduced, leading to simpler structures.

Fig. 2(a) shows the overall configurations of the proposed

Manuscript received October 24th, 2023. This work was supported partly by National Natural Science Foundation of China No.62371089, partly by Dalian Excellent Young Science and Technology Talents Project 2023RY015, and partly by Fundamental Research Funds for the Central Universities DUT23YG111. H. Li, J. Xu, Y. Nan and C. Zhou are with School of

Information and Communication Engineering, Dalian University of Technology, Dalian, 116024, China. Q. Chen is with Research Institute of Electrical Communication, Tohoku University, 980-8577, Japan. (E-mail: hui.li@dlut.edu.cn).

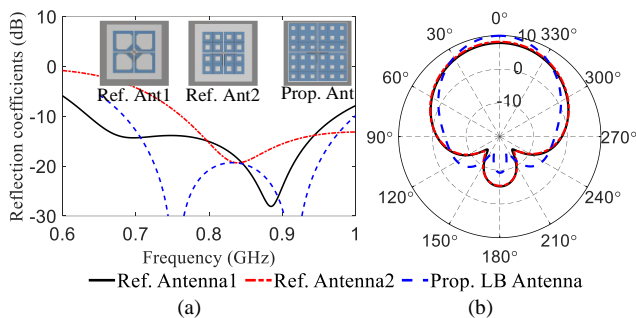


Fig. 5. Evolution of the proposed antennas: (a) reflection coefficients; (b) radiation patterns.

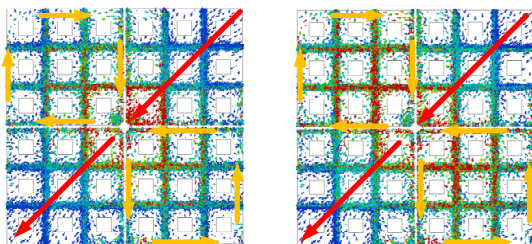


Fig. 6. Surface currents for the dual polarized dipole at (a) 0.7GHz; (b) 1 GHz.

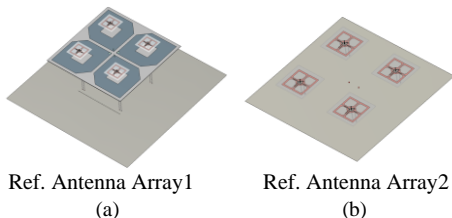


Fig. 7. Reference antenna arrays: (a) original LB-HB antennas without FSS; (b) HB antennas on ideal ground plane.

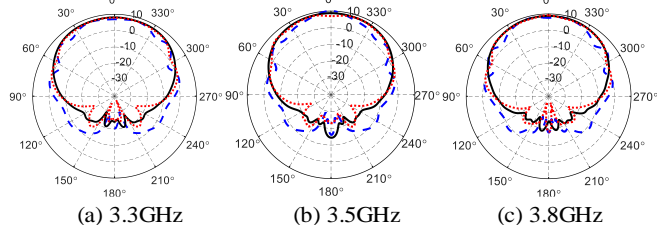


Fig. 8. Radiation patterns of the HB antennas for the reference antenna and the proposed antenna at (a) 3.3 GHz; (b) 3.5 GHz; (c) 3.8 GHz.

(b) on the $\phi = 45^\circ$ plane.

To move down the resonance of the LB antenna to the target band, each loop of the LB radiator is expanded to a 3×3 FSS structure, without changing the size of the FSS unit. Consequently, the resonance is moved back to 0.69-0.96 GHz, as given in Fig. 5(a). The capacitive coupling between the FSS units replaces the capacitive loading of the FSS in [30]. Therefore, the proposed antenna provides good impedance matching though the profile is low. Compared with the reference antennas, the proposed LB antenna provides a higher gain but a narrower 3-dB beamwidth due to larger antenna aperture. The current distributions of the LB FSS-based radiators at 0.7 and 1 GHz are given in Fig. 6.

To investigate the performance of the proposed HB antennas, two other antenna arrays setups are investigated. The first

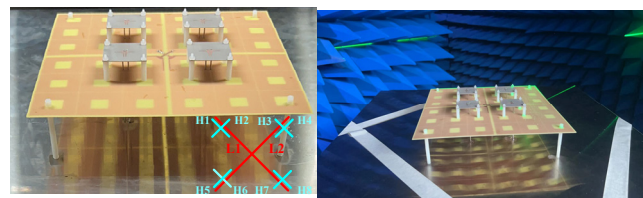


Fig. 9. (a) Antenna prototype; (b) Measurement setup of the proposed base station antenna system.

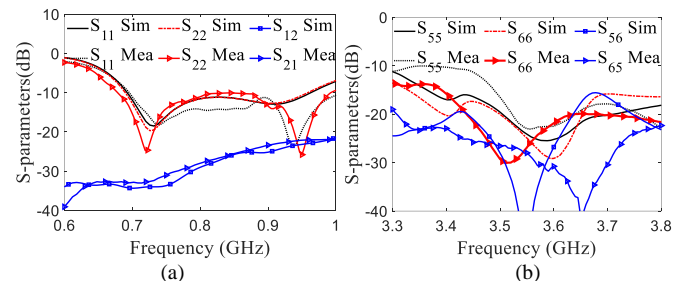


Fig. 10. Simulated and measured S-parameters for the proposed base station antenna system: (a) LB antenna; (b) HB antenna.

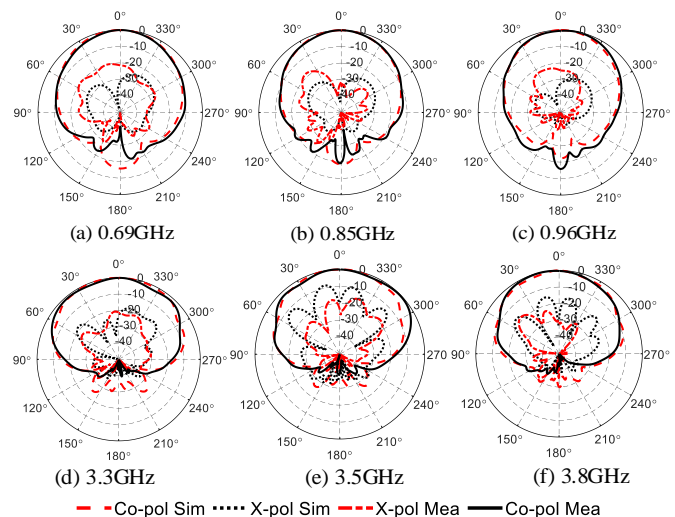


Fig. 11. Measured and simulated radiation patterns of the antenna array.

setup includes the conventional LB and HB antennas on the ground plane without any FSS structure or choke [33], as given in Fig. 7(a). In the second setup, the HB antennas are simply placed above the ground plane, as shown in Fig. 7(b).

Fig. 8 displays the radiation patterns of the HB antennas at different frequencies over the operating band in different setups. Compared with the HB antennas on the ground plane, the radiation pattern of the HB antenna in the first setup is severely distorted by the LB antenna, resulting in a smaller beamwidth and a lower gain. With the proposed LB radiator built from FSS structures, the radiation pattern of the HB antennas has been effectively restored, which is almost identical to that on the ideal ground plane.

The HB antennas above have limited impact on the radiation of the LB antennas, as they are electrically small. When more HB antennas are implemented, pattern distortion would appear due to the mutual coupling between HB antennas.

III. MEASUREMENT RESULTS AND DISCUSSIONS

TABLE I
COMPARISONS WITH OTHER SHARED-APERTURE BASE STATION ANTENNAS

Ref.	Design method	Array size ($\lambda_L \times \lambda_L \times \lambda_L$)*	Double-/Multi-layers	Mea-HPBW (variation)	Bandwidth	Gain (dBi)
[27]	FSS	0.69×0.69×0.14	Multi	5°/25°	0.69-0.96GHz/3.3-3.8GHz	8.3/6.5 dBi
[29]	FSS	1.13×1.13×0.41	Multi	Not Given	1.7-2.4 GHz/3.3-3.8GHz	8/7.2 dBi
[30]	FSS	0.68×0.68×0.14	Multi	14°/40°	0.69-0.96GHz/3.3-4.9GHz	8.8/8.3 dBi
[33]	Filter	0.41×0.41×0.2	Double	10°/11°	0.69-0.96GHz/3.3-3.8GHz	8.7/8.1 dBi
[20]	Filter	0.41×0.41×0.184	Double	5°/16°	0.69-0.96GHz/3.3-3.8GHz	7/10.2 dBi
[17]	Filter	0.5×0.5×0.23	Double	10°/16°	1.9-2.5GHz/3.3-3.9GHz	9.1/7.5 dBi
Prop. Ant.	FSS	0.48×0.48×0.14	Double	8°/14°	0.69-0.96GHz/3.3-3.8GHz	9/8.3 dBi

* λ_L is the free-space wavelength at lowest frequency in LB.

To validate the proposed method, a prototype of the base station antenna array was fabricated and measured, as shown in Fig. 9(a). Air holes were drilled on the substrate of both the LB and the HB antennas, and nylon was used to support the antennas. The simulated and measured S-parameters of the proposed antenna array were presented in Fig. 10, showing good agreements for both the LB and the HB antennas. The measured and simulated bandwidths of the LB antenna with different polarizations covered 0.69-0.96 GHz, as shown in Fig. 10(a). For the HB antennas, port 5 and port 6 were selected as the representatives for demonstration, whose bandwidth covered 3.3-3.8 GHz. The simulated and measured isolations of the LB antenna were above 20 dB, whereas the isolations were above 15 dB for the HB antennas.

The radiation patterns of the antennas were measured in the anechoic chamber, with the measurement setup given in Fig. 9 (b). Fig. 11 showed the radiation patterns of the LB and HB antennas, with representative frequencies selected at 0.69 GHz, 0.85 GHz and 0.96 GHz in the LB, and 3.3 GHz, 3.5 GHz and 3.8 GHz in the HB. Due to the symmetry of the antenna array, only radiation patterns with $\pm 45^\circ$ polarizations (port L1 and port H4) were presented to facilitate a clear comparison between the simulated and measured results. In general, there was a strong agreement between the measured and simulated radiation patterns. As depicted in Fig. 11(a)-(c), the LB antenna maintained a stable radiation pattern across the operating band, with the measured XPD consistently exceeding 20 dB. Furthermore, with the FSS structure serving as the reflector, the HB antenna exhibited a stable unidirectional boresight radiation pattern as well. In the HB, the measured cross-polarization levels were a bit higher than the simulated ones due to the cable influence.

Fig. 12 shows the simulated and measured gains as well as the beamwidth of the LB and HB antennas over the operating band. In the LB, the averaged measured gain was around 0.5 dB lower than the simulated ones, and the measured gain varied within the range of 9 ± 0.3 dBi, which was relatively high and stable. The HPBW ranged from 60° to 68° . In the HB, the measured gains fell in the range of 8.3 ± 0.7 dBi, with the HPBW between 86° and 100° . The stable performances of both antennas make the proposed system suitable for base station applications.

The proposed antennas are compared with the state-of-the-art dual-polarized co-aperture antenna arrays in the literatures in Table I. All the antenna systems under comparison consist of one LB antenna and four HB antennas. In [27], [29] and [30],

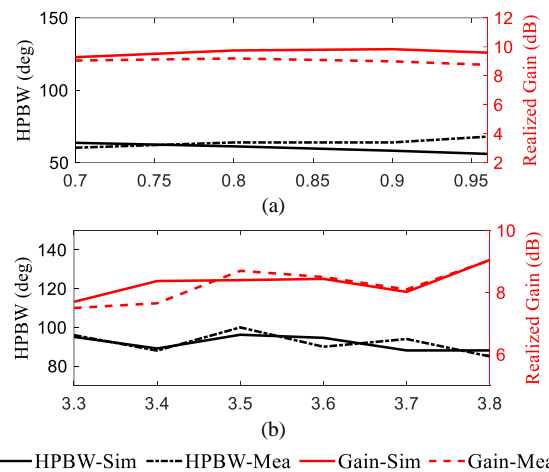


Fig. 12. (a) Measured and simulated realized gains and HPBWs in the LB; (b) Measured and simulated realized gains and HPBWs in the HB.

FSS structures have been utilized between the LB and HB antennas to enhance radiation performance. Despite the increased number of antenna layers, the overall profile has been reduced compared with the antennas with filters structures [17], [20], [33]. Compared with the antennas with intermediate FSS structures, the lateral size of the proposed design and HPBW have been greatly reduced. At the same time, the variations of the HPBW at the high band are significantly improved due to the stable radiation patterns. Compared with the filter-based antennas, although the lateral size of our proposed antenna is slightly larger due to the FSS structure serving as the radiator, a nearly 50% reduction in profile has been achieved while maintaining similar HPBW and gains at both frequency bands. Consequently, the proposed antenna system outperforms the existing schemes in terms of low profile, simple structure and stable radiation patterns.

IV. CONCLUSION

In this letter, a distinct scheme has been proposed for designing co-aperture base station antennas. Unlike conventional cross dipole antennas, FSS structure has been employed as the radiator at the LB, and at the same time as the reflector for the HB antennas. With simply two layers, the HB and LB antennas have been well decoupled without pattern distortion. The gains of the LB antenna and the HB antennas vary within the ranges of 9 ± 0.3 dBi and 8.3 ± 0.7 dBi, respectively, exhibiting stable radiation features. The proposed scheme is suitable for base stations due to its simple structure and outstanding radiation features. In the future, more efforts would be made to reduce the profile of the HB antennas.

REFERENCES

- [1] Gupta and R. K. Jha, "A survey of 5G network: architecture and emerging technologies," *IEEE Access*, vol. 3, pp. 1206-1232, 2015.
- [2] M. Shafi et al., "5G: A tutorial overview of standards, trials, challenges, deployment, and practice," *IEEE J Sel. Areas Commun.* vol. 35, no. 6, pp. 1201-1221, Jun. 2017.
- [3] A. Alieldin, Y. Huang, S. J. Boyes, M. Stanley, S. D. Joseph, and B. Al-Juboori, "A dual-broadband dual-polarized fylfot-shaped antenna for mobile base stations using MIMO over-lapped antenna subarrays," *IEEE Access*, vol. 6, pp. 50260–50271, 2018.
- [4] H. Q. Ngo, E. G. Larsson and T. L. Marzetta, "Energy and spectral Efficiency of very large multiuser MIMO systems," *IEEE Trans. Commun.*, vol. 61, no. 4, pp. 1436-1449, Apr. 2013.
- [5] H. Huang, X. Li, and Y. Liu, "A low-profile, dual-polarized patch antenna for 5G MIMO application," *IEEE Trans. Antennas Propag.*, vol. 67, no. 2, pp. 1275–1279, Feb. 2019.
- [6] H. Huang, X. Li and Y. Liu, "5G MIMO antenna based on vector synthetic mechanism," *IEEE Antennas Wireless Propag Lett.*, vol. 17, no. 6, pp. 1052-1055, Jun. 2018.
- [7] Y. Liu, S. Wang, N. Li, J. -B. Wang and J. Zhao, "A compact dual-band dual-polarized antenna with filtering structures for Sub-6 GHz base station applications," *IEEE Antennas Wireless Propag. Lett.*, vol. 17, no. 10, pp. 1764-1768, Oct. 2018.
- [8] Y. Li, Z. Zhao, Z. Tang and Y. Yin, "Differentially fed, dual-band dual-polarized filtering antenna with high selectivity for 5G Sub-6 GHz base station applications," *IEEE Trans. Antennas Propag.*, vol. 68, no. 4, pp. 3231-3236, Apr. 2020.
- [9] H. Huang, Y. Liu and S. Gong, "A dual-broadband, dual-polarized base station antenna for 2G/3G/4G applications," *IEEE Antennas Wireless Propag. Lett.*, vol. 16, pp. 1111-1114, 2017.
- [10] Y. He, Y. Yue, L. Zhang and Z. N. Chen, "A dual-broadband dual-polarized directional antenna for all-spectrum access base station applications," *IEEE Trans. Antennas Propag.*, vol. 69, no. 4, pp. 1874-1884, Apr. 2021.
- [11] F. Jia, S. Liao and Q. Xue, "A dual-band dual-polarized antenna array arrangement and its application for base station antennas," *IEEE Antennas Wireless Propag. Lett.*, vol. 19, no. 6, pp. 972-976, Jun. 2020.
- [12] R. Wu and Q. X. Chu, "A compact, dual-polarized multiband array for 2G/3G/4G base stations," *IEEE Trans. Antennas Propag.*, vol. 67, no. 4, pp. 2298-2304, Apr. 2019.
- [13] X. Liu et al., "A mutual-coupling-suppressed dual-band dual-polarized base station antenna using multiple folded-dipole antenna," *IEEE Trans. Antennas Propag.*, vol. 70, no. 12, pp. 11582-11594, Dec. 2022.
- [14] L. Y. Nie et al., "A low-profile coplanar dual-polarized and dual-band base station antenna array," *IEEE Trans. Antennas Propag.*, vol. 66, no. 12, pp. 6921-6929, Dec. 2018.
- [15] Y. He, Z. Pan, X. Cheng, Y. He, J. Qiao and M. M. Tentzeris, "A novel dual-band, dual-polarized, miniaturized and low-profile base station antenna," *IEEE Trans. Antennas Propag.*, vol. 63, no. 12, pp. 5399-5408, Dec. 2015.
- [16] Y. Chen, J. Zhao and S. Yang, "A novel stacked antenna configuration and its applications in dual-band shared-aperture base station antenna array designs," *IEEE Trans. Antennas Propag.*, vol. 67, no. 12, pp. 7234-7241, Dec. 2019.
- [17] Y. Da, X. Chen and A. A. Kishk, "In-band mutual coupling suppression in dual-band shared-aperture base station arrays using dielectric block loading," *IEEE Trans. Antennas Propag.*, vol. 70, no. 10, pp. 9270-9281, Oct. 2022.
- [18] X. Lu, Y. Chen, S. Guo and S. Yang, "An electromagnetic-transparent cascade comb dipole antenna for multi-band shared-aperture base station antenna array," *IEEE Trans. Antennas Propag.*, vol. 70, no. 4, pp. 2750-2759, Apr. 2022.
- [19] W. Niu, B. Sun, G. Zhou and Z. Lan, "Dual-band aperture shared antenna array with decreased radiation pattern distortion," *IEEE Trans. Antennas Propag.*, vol. 70, no. 7, pp. 6048-6053, Jul. 2022.
- [20] J. Jiang and Q. -X. Chu, "Dual-band shared-aperture base station antenna array based on 3-D chokes," *IEEE Antennas Wireless Propag. Lett.*, vol. 22, no. 4, pp. 824-828, Apr. 2023.
- [21] S. J. Yang, Y. Yang and X. Y. Zhang, "Low scattering element-based aperture-shared array for multiband base stations," *IEEE Trans. Antennas Propag.*, vol. 69, no. 12, pp. 8315-8324, Dec. 2021.
- [22] S. J. Yang, R. Ma and X. Y. Zhang, "Self-decoupled dual-band dual-polarized aperture-shared antenna array," *IEEE Trans. Antennas Propag.*, vol. 70, no. 6, pp. 4890-4895, Jun. 2022.
- [23] G. N. Zhou, B. H. Sun, Q. -Y. Liang, S. T. Wu, Y. H. Yang and Y. M. Cai, "Triband dual-polarized shared-aperture antenna for 2G/3G/4G/5G base station applications," *IEEE Trans Antennas Propag.*, vol. 69, no. 1, pp. 97-108, Jan. 2021.
- [24] Y. L. Chang and Q. X. Chu, "Suppression of cross-band coupling interference in tri-band shared-aperture base station antenna," *IEEE Trans. Antennas Propag.*, vol. 70, no. 6, pp. 4200-4214, Jun. 2022.
- [25] Y. Li and Q. X. Chu, "Self-decoupled dual-band shared-aperture base station antenna array," *IEEE Trans. Antennas Propag.*, vol. 70, no. 7, pp. 6024-6029, Jul. 2022.
- [26] R. C. Dai, H. Su, S. J. Yang, J. H. Ou and X. Y. Zhang, "Broadband electromagnetic-transparent antenna and its application to aperture-shared dual-band base station array," *IEEE Trans. Antennas Propag.*, vol. 71, no. 1, pp. 180-189, Jan. 2023.
- [27] D. He, Y. Chen and S. Yang, "A low-profile triple-band shared-aperture antenna array for 5G base station applications," *IEEE Trans. Antennas Propag.*, vol. 70, no. 4, pp. 2732-2739, Apr. 2022.
- [28] Y. Zhu, Y. Chen and S. Yang, "Integration of 5G rectangular MIMO antenna array and GSM antenna for dual-band base station applications," *IEEE Access*, vol. 8, pp. 63175-63187, 2020.
- [29] Y. Zhu, Y. Chen and S. Yang, "Cross-band mutual coupling reduction in dual-band base-station antennas with a novel grid frequency selective surface," *IEEE Trans. Antennas Propag.*, vol. 69, no. 12, pp. 8991-8996, Dec. 2021.
- [30] Y. Zhu, Y. Chen and S. Yang, "Decoupling and low-profile design of dual-band dual-polarized base station antennas using frequency-selective surface," *IEEE Trans. Antennas Propag.*, vol. 67, no. 8, pp. 5272-5281, Aug. 2019.
- [31] Q. X. Chu, D. L. Wen and Y. Luo, "A broadband $\pm 45^\circ$ dual-polarized antenna with Y-shaped feeding lines," *IEEE Trans. Antennas Propag.*, vol. 63, no. 2, pp. 483-490, Feb. 2015.
- [32] Z. Bao, Z. Nie and X. Zong, "A novel broadband dual-polarization antenna utilizing strong mutual coupling," *IEEE Trans. Antennas Propag.*, vol. 62, no. 1, pp. 450-454, Jan. 2014.
- [33] Y. Li and Q. X. Chu, "Coplanar dual-band base station antenna array using concept of cavity-backed antennas," *IEEE Trans. Antennas Propag.*, vol. 69, no. 11, pp. 7343-7354, Nov. 2021.